Histochem Cell Biol (2012) 137:377–389
DOI 10.1007/s00418-011-0897-9

ORIGINAL PAPER

STK31(TDRD8) is dynamically regulated throughout mouse spermatogenesis and interacts with MIWI protein

Jianqiang Bao · Li Wang · Jianbo Lei · Yanqin Hu · Yue Liu · Hongbin Shen · Wei Yan · Chen Xu

Accepted: 29 November 2011 / Published online: 29 December 2011

Abstract Tudor-domain-containing proteins (TDRDs) are suggested to be critical regulators of germinal granules assembly involved in Piwi-interacting RNAs (piRNAs)-mediated pathways, of which associated components and the underlying functional mechanisms, however, remain to be elucidated. We herein characterized the expression pattern of STK31, a member of TDRDs subfamily (also termed as TDRD8), throughout spermatogenesis during mouse postnatal development. RT-PCR and Western blot verified its preferential expression in testis, but not in any other somatic tissues, in addition to embryonic stem cells. Immunofluorescent staining demonstrated that STK31 was confined to granules-like structures in mid-to-late spermatocyte cytoplasm and to acrosomal cap starting at steps 7–8 of spermatids. Furthermore, STK31 retained its localization to equatorial segment of acrosome during epididymal maturation, capacitation, and acrosome reaction. Co-immunoprecipitation assay in vivo and in vitro confirmed MIWI is a bona fide partner of STK31 in mice testes, in combination with LC/MS identification. We also discovered a group of heat shock proteins specifically associated with STK31 in vivo. Our findings suggest mouse STK31 could be a potential nuage-associated protein in the cytoplasm of mid-to-late spermatocytes and play pivotal roles related to fertilization.

Keywords STK31 · Spermatogenesis · Equatorial segment · MIWI · Nuage

J. Bao and L. Wang contributed equally to this work.

Electronic supplementary material The online version of this article (doi:10.1007/s00418-011-0897-9) contains supplementary material, which is available to authorized users.

J. Bao · L. Wang · Y. Hu · Y. Liu · C. Xu (✉)
Shanghai Key Laboratory for Reproductive Medicine, Department of Histology and Embryology, Shanghai Jiao Tong University School of Medicine, 280, South Chongqing Road, Shanghai 200025, China
e-mail: chenx@shsmu.edu.cn

J. Lei · H. Shen
Key Laboratory of System Control and Information Processing, Department of Automation, Ministry of Education of China, Shanghai Jiao Tong University, 800 Dongchuan Road, Shanghai 200240, China

W. Yan
Department of Physiology and Cell Biology, University of Nevada Reno, 1664 North Virginia St, CMM, MS0575, Reno, NV 89557, USA

Introduction

In the male, the prerequisite for propagation of species and life continuation is spermatogenesis, during which the interaction between germ cells and their supporting cells-Sertoli cells, is crucial and tightly regulated, and a prominent part of cytoplasmic contents shed by the spermatids, also known as "Residual body (RB)", is eventually phagocytosed by the neighboring Sertoli cells (Hermo et al. 2010). However, spermatozoa generated in the lumen of testicular seminiferous tubules are not motility-competent or able to fertilize the eggs, and instead they must undergo a transit during the epididymal duct, a process known as "epididymal maturation", to acquire motility capability (Cornwall 2009; Sipila et al. 2009). A multitude of post-translational modifications or small molecules exchange may take place during this process so as to endow the motility capability to spermatozoa. Spermatogenesis is a continuous process, taking place in a fashion described as "spermatogenic wave" along the epithelium of seminifer-

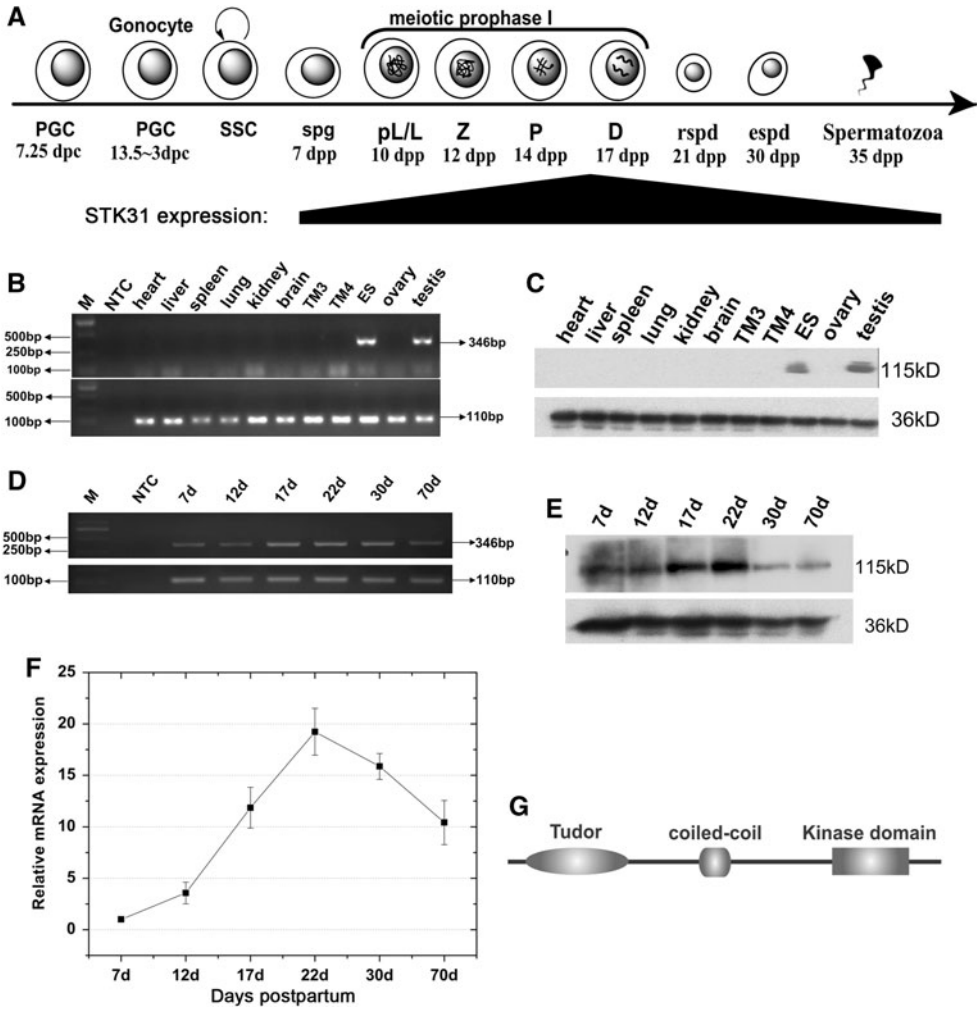

Fig. 1 Expression of stk31 mRNA and protein in multiple tissues and developing testes. **a** A summary of key developmental time points during mouse spermatogenesis (Drumond et al. 2011); *Black shape* represents STK31 expression at corresponding developmental time. **b** RT-PCR detection of stk31 mRNA expression in normal multiple mouse tissues and in cell lines (*TM3* Leydig cell, *TM4* Sertoli cell, *ES* embryonic stem cell line). Only bands were detected in ES cell and testes; **c** Western blot analysis of STK31 protein in multiple organs and cell lines, GAPDH (36 kD) was used as a loading control; **d** RT-PCR detection of stk31 mRNA in developing testes. **e** Western blot analysis of STK31 protein in developing testes. **f** Real time PCR assay of stk31 mRNA level during mouse postnatal development. **g** Schematic illustration of STK31 protein predicted domains. N-terminal Tudor domain and C-terminal Ser/thr kinase domain are separated by a central coiled-coil motif with low complexity. *NTC* non-template control

ous tubules (Lam et al. 1970; Yoshida et al. 2006). According to the distinctive association of germ cells in combination with specific developmental steps of spermatids during spermiogenesis, there are in total XII stages in the cross sections of mouse seminiferous epithelium as described previously (Leblond and Clermont 1952; Oakberg 1956; Russell et al. 1990). During the first wave of spermatogenesis, specific types of germ cell turn up in a well-organized order at special time during prepubertal development in mice (summarized in Fig. 1a) (Drumond et al. 2011). Although a large amount of potential genes, especially testis-specific genes, have been discovered and verified to be essential for spermatogenesis from knockout/transgenic model organisms (Jamsai and O'Bryan 2011), however, the underlying mechanisms orchestrating these testis-intrinsic and external factors responsible for spermatogenesis, in particular spermiogenesis, remain largely unknown (Cheng and Mruk 2011; Yan 2009).

Protein phosphorylation and de-phosphorylation constitute a significant mechanism in signal transduction, a reversible process catalyzed by protein kinases and phosphatases at either serine/threonine residues (serine/threonine kinase) or tyrosine (tyrosine kinase) residues of their substrates. A large body of evidence has showed that abundant protein kinases play critical roles throughout spermatogenesis, and even associate with sperm maturation in the epididymis, capacitation (Ca), acrosome reaction (AR), and sperm–egg binding/fusion. One prominent feature is the co-existence of full-length and truncated form of protein kinases in testes, such as FerT (truncated form of full length Fer kinase) and tr-kit (truncated form of full length kit kinase) (Kierszenbaum 2006). It has been reported that some testis-specific kinases are essential for spermatogenesis and/or fertility, exemplified by TSSK1-6 (testis-specific serine/threonine kinase) family members (Spiridonov et al. 2005a; Xu et al. 2008b; Zuercher et al. 2000). TSSK1-2 were required for functional transformation of chromatoid body (CB) in mouse spermatids (Shang et al. 2010), and their specific substrate, TSKS, also was expressed in the haploid cells, and interacts with TSSK2; Expression of TSSK3 was restricted to interstitial Leydig cells in testes of adult males (Zuercher et al. 2000), whereas TSSK6 (initially named as SSTK), located exclusively to heads of spermatids, interacts with heat shock protein family members,

such as HSP90-1β, HSC70, and HSP70 proteins (Jha et al. 2010). Targeted deletion of TSSK6 led to male infertility due to broad alterations in morphology and motility of spermatozoa, together with abnormal chromatin condensation (Spiridonov et al. 2005b); Sosnik et al. 2009). Protein phosphorylation also plays an important role during meiosis and post-meiotic chromatin remodeling of haploid spermatids (Wu et al. 2000). Given the significance of phosphorylation events in regulating signal transduction and cell–cell communication, it is not surprising that deletion of protein kinases, especially testis-specific kinases, such as TSSK family, could induce abnormal spermatogenesis and male infertility (Sosnik et al. 2009; Xu et al. 2008a).

Tudor-domain containing proteins (TDRD), a subfamily of Tudor family proteins comprise 10 members (TDRD1-9,12) in murine, most have been demonstrated to localize and operate exclusively in the male germ cells and associate with germinal granules (nuage) essential for germline development (Goulet et al. 2008; Tanaka et al. 2011; Yabuta et al. 2011; Yang et al. 2010). PIWI (P-element-induced wimpy testis) family proteins, namely MILI, MIWI, MIWI2 in murine genome, are a subfamily of Argonaute proteins, which have been previously shown as the core components of RNA-induced silencing complex (RISC) in the siRNA-mediated pathway (Carmell et al. 2007; Grivna 2006; Wang et al. 2009). Interestingly, expressions of PIWIs were mostly restricted to germline cells, similar to expression profile of TDRD members. One prominent feature conserved throughout germline development is the formation of germinal granules, also known as nuage, a kind of cytoplasmic non-membrane amorphous aggregate of RNA and proteins with high electron-density around the nucleus. Further investigation showed that germinal granules, commonly sharing similar morphology and molecular components in various animals, are not a static ribonucleoprotein (RNP) compartment, but undergo dynamical remodeling at different spermatogenic stages (Yabuta et al. 2011). Knockout mice resulting in abnormal nuage/CB development elicit male sterility, suggesting they have conserved and significant roles, which, however, remain to be elucidated. TDRD1 forms a complex with MILI localized at the intermitochondrial cements (IMC), termed "pi-body" in fetal prospermatogonia as well as spermatocytes, and interacts with MIWI at Chromatoid body (CB) in spermatids (Barsh et al. 2009). In contrast, TDRD9 co-localized with MIWI2 to a compartment sharing similar components with processing body (GW182 body), termed "piP bodies" (Barsh et al. 2009). It has been proposed that pi-body and piP bodies co-operate with each other in the piRNAs pathway to impart retrotransposons silencing through "Ping-pong" cycle mechanism. Like TDRD1 localization, TDRD2/TDRKH also exhibited granular pattern in the cytoplasm of spermatogonia and meiotic spermatocytes, and yet concentrated into a larger cytoplasmic aggregate in spermatids throughout adulthood (Chen et al. 2009). Moreover, TDRD5/6/7 displayed distinct but overlapping expression distribution at different stages of germ cells (Tanaka et al. 2011; Yabuta et al. 2011). Interestingly, they also co-localized in the IMC and CB with TDRD1 (Tanaka et al. 2011; Vasileva et al. 2009; Yabuta et al. 2011), deficiency of which caused aberrant CB architecture, retrotransposons derepression and male infertility. In contrast, TDRD3 has been shown as a component of cytoplasmic stress granules (SGs) through interacting with Fragile-X syndrome protein (FMRP) (Goulet et al. 2008; Linder et al. 2008; Yang et al. 2010), a well-known protein marker re-localized to SGs in response to various cellular stresses. TDRD4, also known as RNF17, although exhibited as large perinuclear granules in spermatocytes and spermatids, similar to TDRD6, TDRD4 actually did not co-localize with any other TDRD members and appeared to assemble into another new kind of granules, namely RNF17 granule, in germ cells (Pan 2005).

Given the critical roles of nuage involved in germline development, further investigation into nuage-associated constituents and non-coding small RNAs (ncRNAs), together with their interaction network, will facilitate our understanding of biogenesis, transformation, and functional pathway of nuage. Herein, we report the dynamical expression profile of stk31, of which the localization resembled the well-defined granular pattern of other TDRD members, throughout mouse spermatogenesis. We also observed that STK31 retained its localization to equatorial segment (ES) during epididymal transit, even after capacitation and AR, suggesting its key roles at fertilization. In addition, we have identified its bona fide interacting protein partner MIWI, deficiency of which caused haploid spermatids developmental arrest, along with a group of heat shock protein chaperons in vivo.

Materials and methods

Animals, tissues and cell lines

All tissues/organs were prepared from C57/BL6 mice purchased from Shanghai SLAC Laboratory Animal Corporation (http://www.slaccas.com, Shanghai, China). All animals were maintained in a temperature- and humidity-controlled room with free access to food and water at Experimental Animal center located at Shanghai Jiao Tong University School of Medicine (STJUSOM). Mouse ES cell line R1 was a kindly gift from Dr Ying Jin (STJUSOM). 293T cell line was preserved in our Laboratory. Animal use protocol complied with Institutional Animal

Care and Use Committee of Shanghai Jiao Tong University School of Medicine.

Semi-quantitative PCR, real time PCR and Western blot analysis

All procedures were carried out as described previously with minor modification (Bao et al. 2010, 2011). Briefly, total RNA was isolated using TRIzol reagent (Invitrogen), and subsequently reverse-transcribed into first-strand cDNA using PrimeScript RT-PCR kit (TakaRa). Primers used are as follows: For stk31 real time PCR: (STK31-F) GGAACAGTTATTGCTCAGGCT, (STK31-R) TTAGGA TCAGGTTTCTTTGCCTC; For stk31 semi-quantitative PCR: (sense) GCAGGGTGATTCAGAGAGCAGC, (antisense) GCTCGCTGGCTCTCAGATTTGG. A 110-bp PCR fragment of GAPDH was used as an internal control.

For Western blot assay, firstly, total protein was extracted from tissues/cells using RIPA lysis buffer (Beyotime) according to manufacture's protocol. Then the protein lysates (50 μg/lane) were fractionated on 8% SDS-PAGE gel and subsequently transferred onto nitrocellulose membranes (Millipore). After completion of blocking membrane with 5% nonfat dried milk in TBS-T at RT for 1 h, the primary antibody α-STK31 (1:1,000) was added and incubated at 4°C overnight. Then membranes were washed with 0.1 M PBS for 3 times (5 min each), and HRP-conjugated secondary antibody was allowed to incubate for 1 h at RT. An enhanced chemiluminescence detection system (Millipore) was used for visualization of specific protein antigen.

Indirect immunofluorescence (IIF) and Squash staining

Indirect immunofluorescence (IIF) was performed on frozen sections or paraffin-embedded sections as described before (Bao et al. 2011). Briefly, for frozen sections, testes prepared from surgically cervical dislocated adult mice were immediately fixed in 4% PFA for 3 h at RT, and allowed to dehydrate overnight in 15% sucrose at 4°C; Frozen sections of 10 μm thickness were prepared and incubated with blocking buffer (0.01 M PBS, 5% NGS, 0.3% Triton X-100, 5% BSA) at RT for 1 h; Then anti-STK31 (GeneTex, Cat: GTX119718, Rabbit source) polyclonal antibody (1:200 dilution), or together with anti-MVH (BD, Purified Human anti-VASA/DDX4, Ref: 560189) (1:500 dilution) for co-staining, was added and incubated at 4°C overnight, followed by washing in 0.01 M PBS for 3 times; The corresponding secondary antibodies were placed into sections for additional 1 h immuno-reaction at RT, followed by incubation with propidium iodide (PI 1:2,000 dilution) or (DAPI) for 5 min at RT to counterstain the nucleus. The sections are finally dehydrated in 85 and 100% MeOH, followed by mounting using 10 μl of Vectashield media(Vector Laboratory), ready for confocal microscopy scan. The acrosome of sperm was visualized by staining of green-fluorescent Alexa Fluor® 488 conjugate of lectin PNA (Invitrogen, Cat. no. L21409). For paraffin-embedded sections, 5 μm sections were prepared according to standard procedures. For antibody staining, the sections were deparaffinized and then immersed in sodium citrate buffer (pH = 6.0), boiled for 15 min in a microwave oven and placed at RT until they cooled down. Subsequent serum blocking and antibody incubation were the same as immunofluorescence protocol as addressed aforementioned. Squash sections have been prepared as described (Bao et al. 2011) previously with a minor modification. Briefly, a short segment of approx. 0.5 mm of stage-defined seminiferous tubules have been isolated under dissecting microscopy (Kotaja et al. 2004), placed into slides, squeezed with coverslips, and then immediately fixed in 4% PFA at RT for 15 min. These squashed sections were subsequently transferred to −80°C for future use or subject to immunostaining procedures as described above. Images were taken using a laser-scanning confocal microscope (Zeiss, LSM510).

Sperm preparation, capacitation, acrosome reaction

After cervical dislocation of the mice, caudal epididymis were collected and placed in 1 ml of PBS solution or M16 medium followed by simply cutting using a scissor to allow sperm "swimming up". The top layer of sperm released in the medium during 15 min incubation were collected and re-suspended. Sperm density was determined using a hematocytometer set at 1–2 × 10^6/ml. Then sperm in the PBS group were directly mounted onto slides and air-dried at RT. For capacitation, M16 medium containing motile sperm was conditioned with 5% BSA and allowed to stand at 37°C for 3 h, whereas 5 μM Ca^{2+} ionophore A23187 was added into M16 medium to induce AR by incubation at 37°C for 3 h. The integrity of acrosome was subsequently examined by staining of Alexa 488-PNA (1:200, Molecular Probes).

Plasmids

pIRES-myc and pIRES-flag plasmids kindly offered by Dr Xuemei Tong are modified versions of pIRESpuro vector (Clontech, Catalog #6031-1) through insertion of two epitope-tag sequence with myc tag (GCCACCATGGAGCA GAAACTCATCTCTGAAGAGGATCTGGGCGAGCAG AAACTCATCTCTGAATAGGATCTG) and flag tag (GC CACCATGGATTACAAGGATGACGACGATAAGGGC GATTACAAGGATGACGACGATAAGGGCGGCGGCG GA) into NheI and Hind III restriction enzymatic sites, respectively. Both mouse stk31 cDNA clone (clone ID: 8861008)

and Miwi(piwiL1) cDNA clone (Clone ID: 40109793) were purchased from Source Bioscience. The full length open reading frames (ORF) for stk31 and miwi were amplified by RT-PCR, gel-purified, digested, and eventually inserted in-frame into BamHI and EcoRV restriction sites, respectively, located in multiple cloning sites (MCS) of their corresponding vectors. The resultant recombinant plasmids containing fragment of ORFs for stk31 and Miwi were named pIRES-Myc-stk31 and pIRES-Flag-Miwi, respectively. All constructs were subject to sequencing to ensure mutation-free and in-frame inserted.

Co-immunoprecipitation and kinase assay

In vivo and in vitro Co-immunoprecipitation analyses were performed as addressed previously (Bao et al. 2010), with a slight modification. Briefly, prepare lysates of testes or plasmids-transfected cells on ice at first, followed by centrifuge at 15,000*g* for 10 min. Then preclear the lysate by adding 40 µl protein G-coupled beads per 1000 µl lysate (Beyotime, Cat: P2009) and discard the beads after centrifuge at 15,000*g* for 20 s. Keep 50 µl lysate as input. Aliquot the remaining precleared lysate: one is for IgG control (4 µg IgG per 500 µl lysate), another is for anti-STK31(GeneTex, Cat: GTX119718) or anti-Myc/Flag (Beyotime, anti-Myc mAb Cat:AM926; anti-Flag mAb Cat:AF519) antibodies (4 µg antibody per 500 µl lysate). After the overnight incubation of those antibodies at 4°C with 80 rpm shaking, 50 µl protein G-beads were added and allowed to shake for additional 3 h. Finally, the beads would be recovered by centrifugation and washed for four times with lysis buffer. The resultant eluent from the beads approx. 25 µl was loaded to the gel together with 5× sample buffer using 1 ml syringe. Subsequent standard Western blot procedures were performed as stated above. All the operations were performed either at 4°C or on ice so as to prevent protein degradation.

Protein kinase assay was performed using ADP-Glo™ Kinase Assay kit (Promega, Cat: V9101) according to manufacture's protocol). Briefly, kinase reaction was performed in a 25-µl reaction buffer using 96-well plates after collecting immunoprecipitants prepared from Myc-Stk31-transfected 293T cells. Subsequently, 25 µl of ADP-Glo™ Reagent was added to allow ATP–ADP conversion, followed by incubation with additional 50 µl Kinase Detection Reagent. In the end, the luminescence was measured with a plate-reading luminometer (PerkinElmer, LS-50).

Mass spectrometry

In brief, trypsinization of excised gel bands and analysis of peptides by liquid chromatograph-mass spectrometry (LC–MS) were performed as described previously (Spiridonov et al. 2005b). Proteins were identified by searching the resultant spectrum of peptides against non-redundant IPI.MOUSE.v3.65.fasta database; X correlation scores above 2.5 were considered reliable.

Results

Stk31 homolog encodes a conserved multidomain protein

Data obtained from the UCSC Genome Brower (Mouse July 2007 [NCBI37/mm9] assembly) revealed that the mouse stk31 gene consists of 24 exons spanning a region of 73.9 kb genomic DNA on chromosome 6qB2.3. All splicing junctions conform to the GU-AG general consensus except intron 5 with GC instead of GU. The resulting mRNA transcript is 3238 bp (GenBank accession no. NM_029916) encoding a large protein (1018aa) with a calculated molecular mass ~115 kD and isoelectric point 5.05. Sequence analyses of amino acids of primary structure provided by the Conserved Domains Database (CDD) and the Protein Family (Pfam version 25.0) database suggest that it is a multidomain protein (modular protein) containing a typical N-terminal "Tudor" domain for recognition of arginine-methylated motifs, a coiled-coil region, and a C-terminal serine/threonine kinase domain (Fig. 1g; Online Resource 1 Fig. 1). Representative domain sequences predicted were highlighted in different color (Online Resource 1 Fig. 2). Stk31 gene was firstly reported as a member of Tudor-domain containing protein (TDRD) family (TDRD1-9, 12) which usually contains at least one "Tudor" motif demonstrated to bind asymmetric dimethylarginine (aDMA) or symmetric dimethylarginine (sDMA) (Cheng et al. 2007, 2009). According to the amino acids sequence, the phylogenetic tree between TDRD members has been constructed as shown in Online Resource 1 Fig. 3, from which we can infer that stk31(TDRD8) has a much closer relationship with TDRD12, suggesting stk31 may have similar function to TDRD12, of which the role remains elusive as yet. Protein sequence alignment of STK31 was presented in Online Resource 1 Fig. 6, and high identity percentage and similarities were observed (Online Resource 1 Figs. 4, 5) between different species, reminiscent of its pivotal roles during evolution of species.

Stk31 mRNA and protein are preferentially and dynamically expressed throughout mouse spermatogenesis

No evidence was available concerning the spatial and temporal distribution of stk31 in mice. Here, through RT-PCR assay (Fig. 1b), we clearly demonstrated that stk31 mRNA is only actively transcribed in testis organ, but not in other

tissues, among multiple organs in adult mice. Intriguingly, there is a notable expression of stk31 mRNA in ES cells which is beyond our expectation (Fig. 1b). Consistent with mRNA expression result, using Western blotting assay, stk31 protein also expressed only in testis and ES cells among tissues analyzed by RT-PCR (Fig. 1c). In addition, no transcripts or STK31 protein bands were detected in TM3 (Leydig cell line) and TM4 (Sertoli cell line) (Fig. 1b), suggesting germ cell-specific expression of stk31 in testis.

To further consolidate these data, we have examined bioGPS (http://bioGPS.org) which is an online integral database including gene and protein function for free extensible and customizable gene annotation portal. In human (GeneAtlas U133A,gcrma at bioGPS), STK31 expression is solely restricted to testicular cells with background level expression of STK31 in other tissues. Similarly, in mouse (GeneAtlas MOE430,gcrma at bioGPS), we can see obviously strong expression of stk31 in testis in addition to relatively low level expression of stk31 in embryonic stem cells and placenta, with no expression observed in other organs. Those data were basically in accordance with our RT-PCR result, hence, stk31 is preferentially expressed in germ cells of testes. To further explore the temporal distribution of stk31, we still performed RT-PCR and Western assay using developing testis both at mRNA and protein level. As shown in Fig. 1d, stk31 mRNA can be detected at 7 days post partum (dpp), with gradual increase until 20dpp and then decrease. Consistently, its protein alteration is in agreement with mRNA level changing tendency (Fig. 1e). The levels of stk31 mRNA and protein peak at 20dpp when testicular germ cells proceed to secondary meiotic spermatocytes. Since no haploid round spermatids emerge and spermatocytes are the predominant cell types in mouse testes before 20dpp during first wave of spermatogenesis (Fig. 1a), the increased level of stk31 mRNA and protein suggests it is most expressed in spermatocytes of mouse testicular cells. We next performed real time PCR (qPCR) to quantify the stk31 mRNA expression in the developing testes, as shown in Fig. 1f, it also revealed that stk31 mRNA is present at 7dpp and is mostly expressed at 22dpp with a relative decreased expression level during subsequent growth, which corresponds to the results above.

Dynamical cellular localization of STK31 during mouse spermatogenesis

Mouse stk31 gene has only been previously reported to be expressed in spermatogonia of mouse testes (Wang et al. 2001). Here, we next examined the overall expression profile of STK31 in adult mice testes using indirect immunofluorescence. STK31 antibody against a short stretch of amino acid residues in the C-terminus of mouse STK31 had been tested to be specific, as there was a single band of ~115 kD on immunoblot (IB) performed using 293T cells transfected with Myc-tagged full length STK31 mRNA construct, while no bands were detected in mock transfection control (Data not shown). IIF showed that, STK31 appeared to be predominantly expressed in the cytoplasm of spermatocytes (Fig. 2A1, arrowheads denoted by spc) at different stages (Fig. 2A2, A4), coinciding with RT-PCR and qPCR results above. Weak expression can be detected in round spermatids (rspd) (Fig. 2, panel A2, arrowheads) compared to its expression level in spermatocytes, suggesting the up-regulated expression of STK31 in pachytene spermatocytes during meiosis. Consistent with previous report, there is also cytoplasmic staining of STK31 in the spermatogonia (spg) (A or B type) (Wang et al. 2001) (Fig. 2A4, arrowheads), however, of which the protein level is much lower than that of spermatocytes and spermatids. Strikingly, we always observed by far the strongest expression of STK31 toward the center of the seminiferous tubules between stage VII and VIII, when elongating spermatids (steps 8–14) have progressed into elongated spermatids (steps 15–16) (Fig. 2A3). Consistently, when we carried out immunostaining of paraffin-embedded sections as shown in Online Resource 1 Fig. 7, even the staining signal of spermatocytes becomes very weak due to the antigen mask/destroy during multiple steps in making paraffin sections, STK31 protein also exhibited the highest expression level towards the lumen of tubules between stages VII and VIII, but was not present at any other stages. Given residual body (RB), the excessive cytoplasm of spermatids which would be eliminated during spermiogenesis, was only present between stages VII and VIII, it is tempting to speculate that part of STK31 protein may relocalized to RB at stages VII–VIII, and finally was engulfed and degraded by the neighboring Sertoli cells. Here we are not clear whether STK31 was expressed in elongating/elongated spermatids or not, due to the resolution limitation (Fig. 2a). To further confirm this, we next performed immunofluorescence staining using squashed sections, which allow single cells to be stained in a mono-layer cross section as described in "Materials and methods". Obviously, in addition to strong cytoplasmic staining signal for spermatocytes, there was also distinct moon-shaped staining around anterior heads of spermatids (Fig. 2b, arrowheads denoted by espd), suggesting STK31 localized to acrosomal region of elongating/elongated spermatid heads. In summary, STK31 was most abundantly expressed in spermatocyte cytoplasm whereas relatively lower level expression was observed in spermatogonia and spermatids as illustrated in Fig. 1a, in adult mice testes.

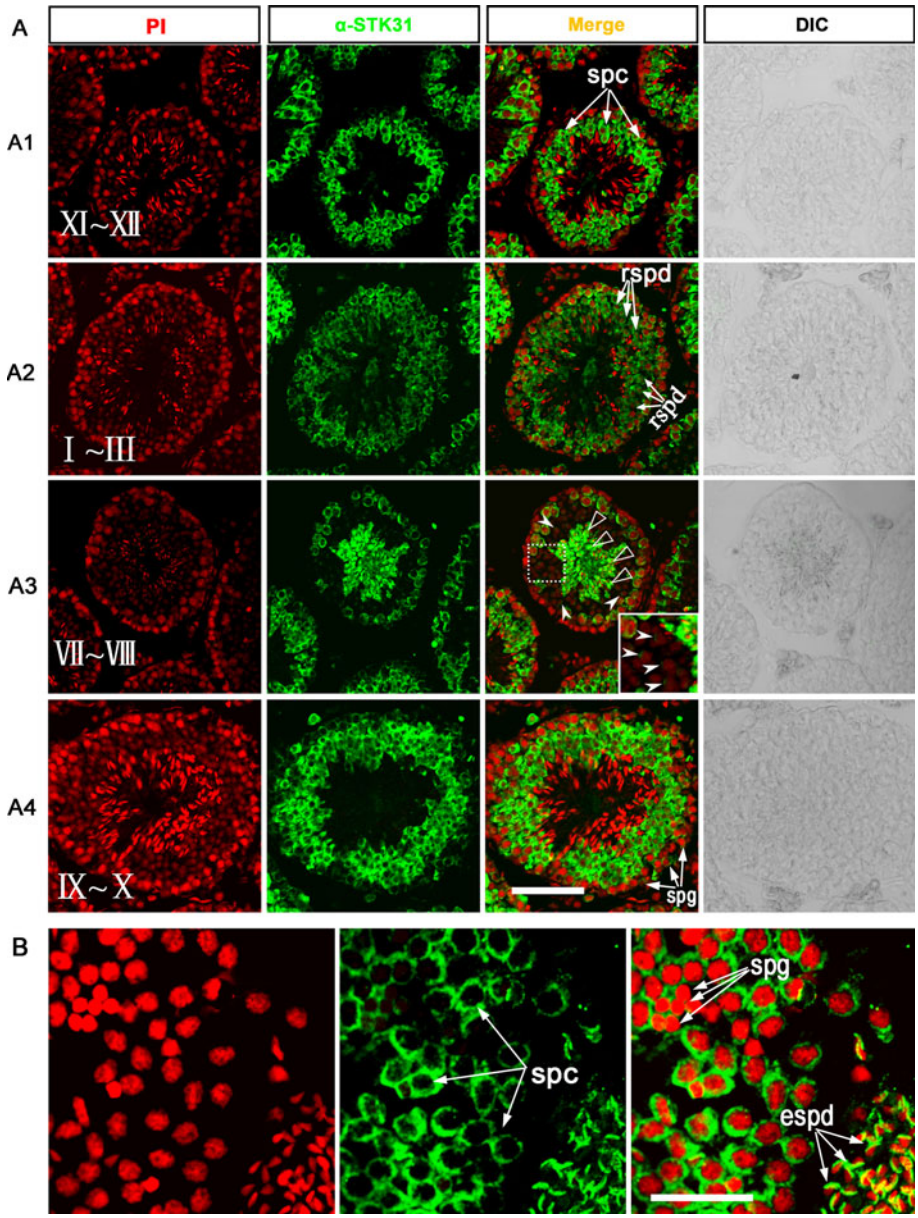

Fig. 2 Immunofluorescent localization of STK31 protein at different stages of adult mouse seminiferous tubules. Nuclear DNA was counterstained with PI (*red*). Cell types of STK31 cytoplasmic localization were indicated by *arrows* (**a**). Stages of different seminiferous epithelial cycles were denoted in Roman numerals in each panel (**a**). *Arrowheads* point to Golgi region of cap-phase elongating spermatids in close vicinity of nuclear rim, whereas open arrowheads (A3) indicate strong staining signal located toward the lumen of only stage VII–VIII tubules. Inset is a high-power magnification of boxed area. **b** STK31 immunostaining of squash cryosections of adult mouse seminiferous tubules. STK31 was abundantly present in acrosome of elongating/elongated spermatids (*arrows* with espd) as well as the cytoplasm of spermatocytes (*arrows* with spc). Nuclear DNA was counterstained with PI (*red*) *Spg* spermatogonia, *spc* spermatocyte, *spd* spermatid, *espd* elongating spermatids, *RB* residual body; (scale bar in **a**, 50 μm; scale bar in **b**, 60 μm)

STK31 localized to granule-like structures in the cytoplasm of mid-to-late spermatocytes and started to aggregate into acrosome at steps 7–8 of spermatids

Previous evidence showed the broad presence of cytoplasmic germinal granules comprised of TDRDs members and PIWI members, as well as germline-associated proteins (Goulet et al. 2008; Moser and Fritzler 2010; Pan 2005; Tanaka et al. 2011; Yabuta et al. 2011). Therefore, we further examined the accurate cytoplasmic staining of STK31 in adult mice testes using high-power magnification microscopy. Interestingly, there appeared to be some granules distributed in cytoplasm of spermatocytes (Fig. 3b, arrows), similar to the granular staining of MVH (Fig. 3b), a germ cell marker concentrated in nuage in spermatocytes and spermatids. To further confirm this, we next performed the co-staining of STK31 and MVH proteins. As shown in Fig. 3b, STK31 exhibits apparent granule-like signals (arrows) in the spermatocytes as observed for MVH, suggesting STK31 also localizes to intermitochondrial cement (nuage) among mitochondrial clusters in spermatocytes. However, we did not notice any granular staining in stages I–VI (Fig. 3a), but apparently they were present in subsequent stages, indicating the preferential confinement of STK31 to germinal granules in mid-to-late spermatocytes. At the lower magnification level, there appeared to be a weak staining resembling the acrosomal vesicles structure (Fig. 2A3, arrowheads) at steps 7–8 spermatids. To further explore this location, we next carried out double Immunofluorescent staining of STK31 and Alexa 488-PNA

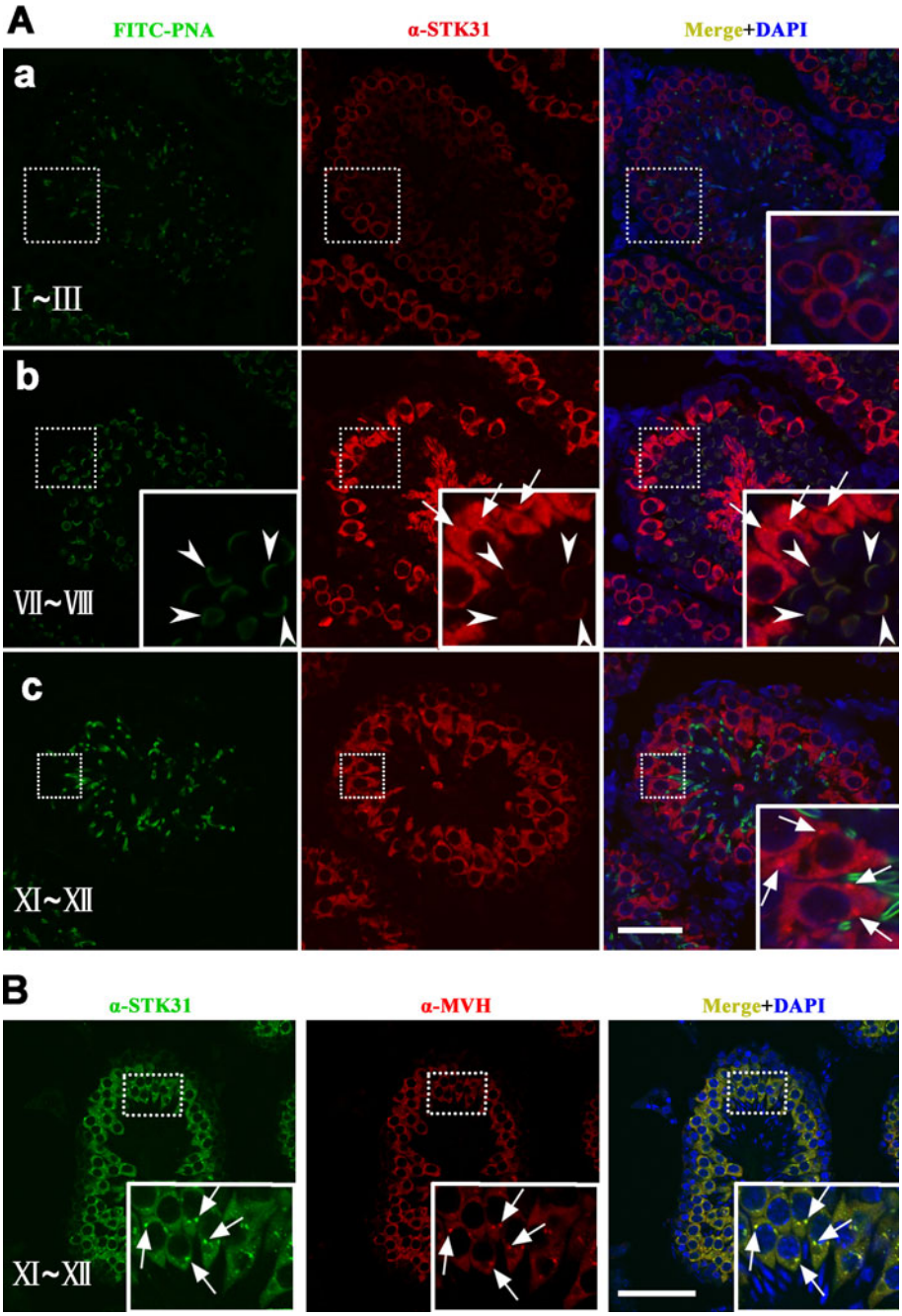

Fig. 3 STK31 exhibited subcellular granular distributions in cytoplasm of mid-to-late pachytene spermatocytes (spc) and aggregated into acrosome beginning at stages VII–VIII. Using indirect immunofluorescence staining, STK31 (*red*) was present specifically in the cytoplasm of germ cells (**a**) at different stages. No granular pattern was observed in the cytosol of germ cells at stages I–II(a), whereas dot-like cytoplasmic granules were detected at stages VII–VIII in spermatocytes (*arrows* in **b**), especially prominent at stages XI–XII (*arrows* in **c**). By co-staining STK31 (*red*) and acrosome (Alexa 488-PNA), STK31 disappeared in the cytoplasm but re-localized to acrosome at stages VII–VIII when acrosomal cap covers more than 1/3 of nuclear membrane surface of steps 7–8 spermatids (*arrowheads* in **b**). **b** Co-localization of STK31 immunostaining with MVH (mouse Vasa homolog). STK31 exhibits similar expression pattern as observed for MVH protein in testicular cells of adult mice, especially colocalizing to the granule-like spots (namely intermitochondrial cements as indicated by *arrows*) present in the spermatocytes. Cell nucleus DNA was counterstained by DAPI (*blue*). Insets are magnified region of corresponding *dashed box* in each panel. (*Scale bar* in **a**, 40 μm; *scale bar* in **b**, 20 μm.)

(specific for acrosomal glycoprotein) using oil microscopy confocal scanning. Surprisingly, α-STK31 completely co-localized with Alexa 488-PNA staining signals (Fig. 3b, arrowheads), suggesting STK31 localized to acrosomal cap of steps 7–8 spermatids which were undergoing transition from the cap phase to elongation phase (acrosome phase) in mice. Furthermore, during subsequent steps of spermatid development, STK31 retained its localization to posterior acrosome compartment (equatorial segment) (Fig. 2b).

STK31 retained its localization to equatorial segment (ES) region during epididymal maturation, capacitation, acrosome reaction (AR)

Since the unique localization of STK31 to acrosome of elongating spermatids as described above, we were interested to further explore if it was still present in the mature spermatozoa during transit of epididymis, capacitation, and AR. As demonstrated in Fig. 4, spermatozoa retrieved from caudal of epididymis revealed an intact acrosome (green)

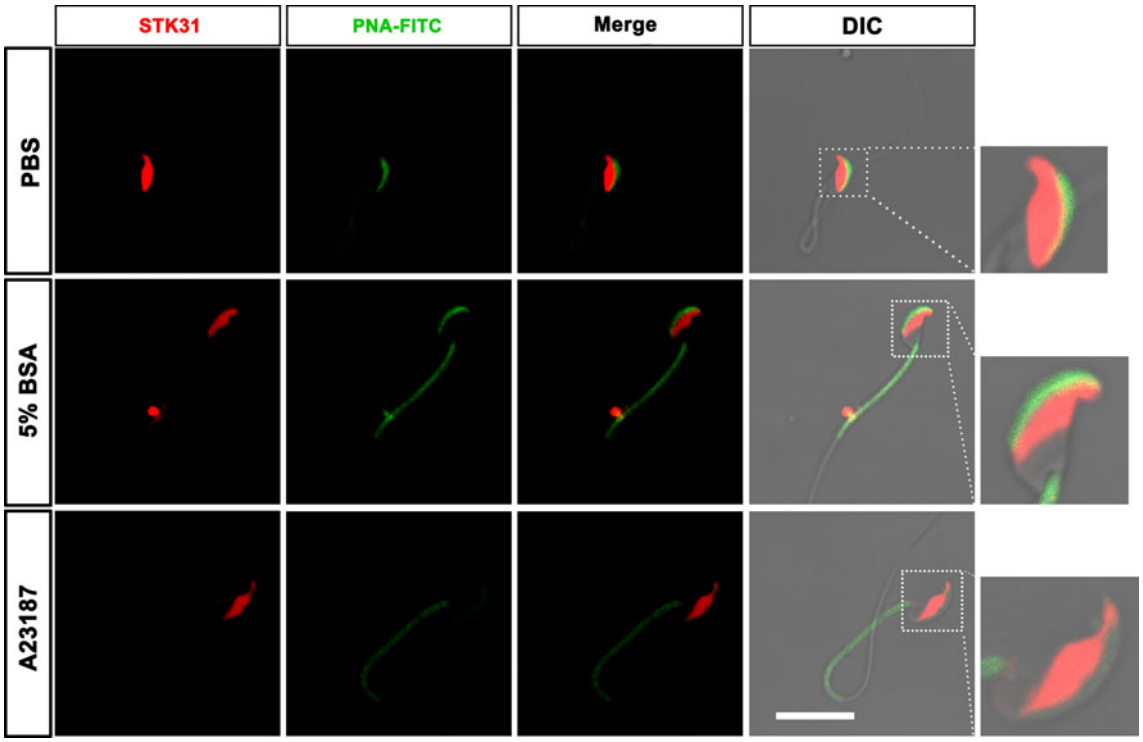

Fig. 4 STK31 localizes to equatorial segment (ES) during transition of epididymal duct, and retains its localization during capacitation and acrosome reaction (AR) using indirect immunofluorescence (IIF). In the PBS group (*upper panel*), STK31 (*red*) clearly localized to equatorial segment, a posterior region of acrosome close to anterior acrosome (cap) which was characterized by Alexa 488-PNA (*green*). After capacitation (5% BSA, middle panel) and AR (A23187, *lower panel*), STK31 always retains its location at posterior AR. *Insets* are magnified area of corresponding dashed box in each panel. (*Scale bar* 10 μm)

and a strong STK31 staining (Fig. 4, PBS group in upper panel). By inspecting high-power magnification of spermatozoa head (Fig. 4, boxed area), we can clearly see that STK31 localizes to the ES of mature spermatozoa. Intriguingly, even after capacitation and AR induced by 5% BSA (Fig. 4, middle panel) and 10 μM A23187 (Fig. 4, lower panel), respectively, STK31 immuno-staining signal was retained restricted to the subcellular ES compartment of spermatozoa heads, suggesting a distinct role from SPESP1, an ES protein which disappeared after AR (Fujihara et al. 2010). Additionally, we demonstrated its protein kinase activity of stk31 as shown in Fig. 5b, combined with its exclusive localization to the ES, presumably indicating its correlation with sperm function.

Identification of STK31-interacting proteins and/or kinase substrates in vivo

Tudor domain, defined by a very conserved stretch of amino acids initially found in Drosophila, has been demonstrated to broadly interact with symmetrically dimethylarginine (sDMA) located in PIWI proteins (Chen et al. 2009; Vagin et al. 2009), suggesting STK31 may operate in similar manner in mouse testis. Hence, we next attempted to investigate the possible interactors or kinase substrates of STK31 by virtue of in vivo Co-immunoprecipitation (Co-IP) assay, in combination with Liquid chromatography–Mass spectrometry (LC–MS) identification, in adult testes. As shown in Fig. 5a (a representative image which has been repeated at least three times), STK31 antibody can specifically recognize three differential bands (Bands 1–3), whereas low-to-indiscernible protein signal of their counterparts were present in the IgG control group, demonstrating the proteins in those three bands may interact directly/indirectly with STK31 during normal spermatogenesis. By means of LC–MS identification, Band 1 was validated as STK31 protein pulled-down specifically by its antibody with a ~115 kD size (Table 1). However, three proteins were identified in Band 2 composed of MIWI, DDX4 (MVH) (a germ cell specific marker), and CUL3 (an Ubiquitin E3 ligase). Attractively, Band 3 has been identified to exclusively comprise a batch of heat shock proteins, including HSPA9, HSPA8, HSPA1B, and testis-specific HSPA2 (Table 1).

STK31 interacts with MIWI protein in vitro

Previous studies showed MIWI protein is exclusively present in the cytosol of pachytene spermatocytes and of round spermatids during mouse spermatogenesis, whereas other

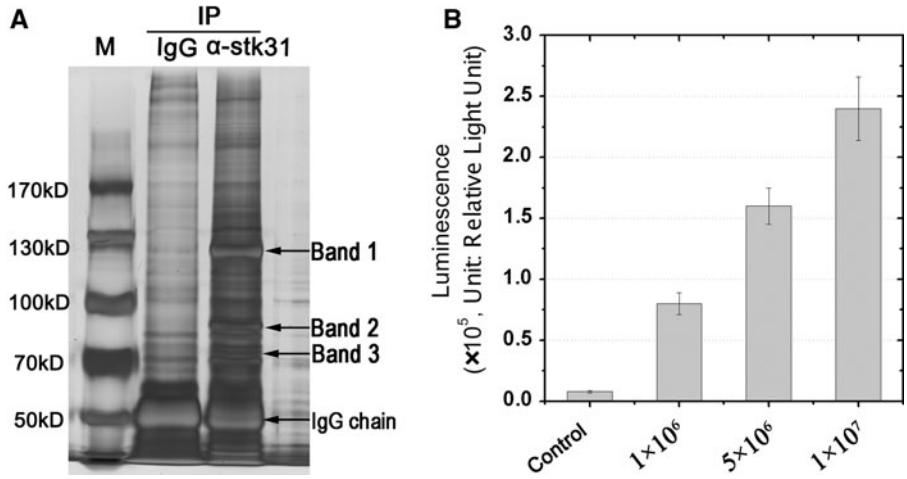

Fig. 5 Identification of STK31-interacting protein partners in testes in vivo and STK31 kinase assay. Using normal Goat-derived IgG as a control, α-stk31 antibody could clearly immunoprecipitated three specific protein bands (**a**) visualized by silver staining following SDS-PAGE, compared to IgG lane, using mouse testes whole lysate. The protein components of each band subsequently identified by LC–MS were listed as Table 1. This experiment had been repeated for at least three times and **a** is a representative image by silver visualization. **b** Protein kinase assay using ADP-Glo™ Kinase Assay kit (Promega). A negative control performed using a normal Goat-derived IgG pulled-down immunoprecipitants showed background luminescence, whereas α-Myc antibody co-immunoprecipitants exhibited obvious luminescence, of which strength was in proportion with amount of pulled-down STK31 protein. *X* axis represents the number of 293T cells transfected with myc-stk31 plasmid

Table 1 Protein components present in co-immunoprecipitants of STK31 identified by LC–MS

MS sample name	Protein name	Protein identification probability (%)	Number of unique peptides	Percentage sequence coverage (%)
Band 1	STK31	100.00	80	73.40
Band 2	DDX4	100.00	12	19.10
Band 2	PIWIL1	100.00	19	25.90
Band 2	CUL3	100.00	8	8.46
Band 3	HSPA9	100.00	13	25.30
Band 3	HSPA8	100.00	23	41.60
Band 3	HSPA1B	99.80	2	11.80
Band 3	HSPA2	100.00	12	35.70

two members of mouse PIWI subfamily, namely MILI and MIWI2, express much earlier in the mouse germline (MILI at E12.5 and MIWI2 in prospermatogonia). Moreover, bodies of evidence showed TDRD members mostly interact with PIWI members by recognizing symmetrically dimethylated arginine (sDMA). Given STK31 is most highly expressed in the cytoplasm of spermatocytes described above, it is conceivable to posit that STK31 and MIWI may interact with each other. To further validate this hypothesis, we made two full-length constructs: Myc-tagged stk31 and Flag-tagged Miwi. Co-immunoprecipitation assay, using either anti-Myc or anti-Flag antibody to pull down lysates prepared from co-transfected 293T cells, unambiguously uncovered that both STK31 and MIWI were able to interact with each other directly in vitro (Fig. 6). This result is consistent with our previous data from testes in vivo co-immunoprecipitation assay, suggesting MIWI is a bona fide STK31 interacting partner.

Discussion

Recently, Tudor-domain containing proteins (TDRDs), a subfamily of conserved TUDOR superfamily proteins which are present in all eukaryotes, most have been found to localize to germinal granules in mouse and drosophila. Strikingly, animals deficient in Tdrd genes exhibited severe developmental abnormalities of nuage (including structure and components), spermatogenic arrest, and derepression of retrotransposons, resulting in male fertility. PIWI proteins, containing MILI (MGI: PIWIL2), MIWI (MGI:PIWIL1), MIWI2 (MGI:PIWIL4) in mice, are a sub-

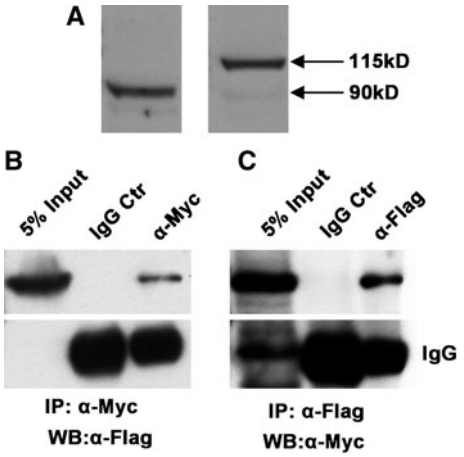

Fig. 6 Co-immunoprecipitation analyses of Myc-stk31 and Flag-piwil1 constructs in vitro. Western blot demonstrated that 293T cells transfected with Myc-stk31 and Flag-piwil1 plasmids expressed both STK31 and PIWIL1 proteins, corresponding to 115 and 90 kD, respectively (**a**). Protein complex prepared from α-Myc immunoprecipitants can be detected with α-Flag antibody using 293T cells (**b**); In turn, α-Flag antibody co-immunoprecipitated proteins contain Myc-tagged STK31 as demonstrated by Western blot (**c**). IgG antibody was used as an internal control

class of Argonaute family proteins, which have been shown previously to preferentially express in male testes and are associated with PIWI-interacting RNAs (piRNAs)-mediated pathway, of which functions are mainly involved in transposons repression through "Ping-pong" cycle mechanism. PIWI knockout mice exhibited severely defective phenotypes, as occurred in most TDRD members knockout mice, reminiscent of their interplay in vivo and shared, but non-redundant, functional pathways during germline development.

Herein, we report in detail, for the first time, the postnatal expression profile of a potential nuage-associated protein, STK31, also named TDRD8, belonging to Tudor-domain containing protein (TDRD) family, in mice. Stk31 gene was initially identified by a systematic screening of genes expressed in mouse spermatogonia through "cDNA subtraction" approach in mice testes (Wang et al. 2001). Consistent with this report, our finding also revealed that expression of stk31 was restricted to germ cells of mouse testes, but not in somatic cells or other organs, in addition to ES cells. Another group recently reported the characterization of stk31 in equine testes by screening equine cDNA library (Sabeur et al. 2008). They found that equine STK31 was specifically expressed in post-meiotic haploid cells, particularly prominent at Golgi region of cap-phase elongating spermatids and at ES of elongated spermatids and mature sperm by immunolocalization probed with STK31 antibody, but not in any other cell types. In agreement with this report, our immunofluorescent staining also revealed that STK31 was confined to Golgi region of early elongating spermatids, and subsequently to acrosome (equatorial region) at elongated spermatids and mature sperm. However, our immunolabeling evidence also unveiled that mouse STK31 was mostly expressed in cytosol of spermatocytes (Fig. 2A1), with conspicuously decreased expression in spermatogonia and round spermatids (Fig. 2A2), indicative of a down-regulated stk31 mRNA transcription or high STK31 protein turnover rate in haploid cells. This is probably due to CUL3-directed Ubquitin-protease pathway, in which CUL3 function as an E3 ligase exclusively expressed in post-meiotic cells (Wang 2005), a supposition supported by our observation that STK31 associated with CUL3 in vivo from our co-immunoprecipitation assay in combination with LC/MS (Table 1).

Intriguingly, in accordance with our expectation, STK31 also exhibited granular localization dispersed in the cytoplasm of mid-to-late spermatocytes, a pattern often found in immunostaining of nuage-associated proteins, such as MVH, in germ cells, implying STK31 may participate in nuage-related pathways (Fig. 3). By Co-immunoprecipitation assay, we demonstrated that MIWI, a member of PIWI subfamily which generally binds transposon-derived piRNAs, is a bona fide interacting partner of STK31 in vitro and in vivo in mice testes, indicating that STK31 is most likely to be involved in piRNAs-mediated transposon control occurring in the germinal granules. Accordingly, our data from Mass Spectrometry (MS) also validated the existence of MVH in α-STK31 pull-down immunoprecipitants, indictive of the possible interaction between STK31 and MVH.

It has been recently suggested that TDRDs are more likely to operate as scaffolding proteins to which a variety of associated factors are recruited and assembled, resulting in the formation of supramolecular complexes (Goulet et al. 2008; Tanaka et al. 2011; Yabuta et al. 2011). Interestingly, most TDRD proteins possess additional modules or motifs in addition to at least one Tudor domain. For example, TDRD1 has four Tudor domains along with a MYND zinc finger motif (Chuma et al. 2006); whereas TDRD9 contains only one Tudor domain plus a DExH RNA helicase domain, suggesting they may be involved in other functional pathways. Likewise, STK31 also possesses a featured serine/threonine protein kinase domain defined by the presence of approx. 250 amino acids located in the C-terminus. Although a large number of serine/threonine kinases and tyrosine kinases have been discovered in mammals, including mice and human, nevertheless, only a handful of testes-specific kinases have been characterized, such as TSSK family (Sosnik et al. 2009; Spiridonov et al. 2005b; Xu et al. 2008b). Bodies of evidence confirmed that protein kinases are of great significance involved in process of spermatogenesis, such as spermatogonial mitosis, meiosis, spermatogenesis, even are connected with capacitation,

AR, and fertilization. Our data showed that STK31 could unambiguously catalyze the phosphorylation of MBP, a protein commonly used as the substrate for kinase assay (Spiridonov et al. 2005a). Attractively, starting at steps 7–8 when Golgi complex aggregates into cap-like pro-acrosome vesicles covering nuclear rim of elongating spermatids, STK31 protein disappeared in the cytosol and specifically localized to acrosome. During late steps of spermiogenesis, STK31 may gradually re-localized to posterior acrosome region, that is, ES, a very significant compartment of sperm head believed to be tightly associated with sperm–oocyte fusion. Furthermore, we showed that STK31 retained its localization to ES during processes of epididymal maturation, capacitation, and even AR (Fig. 4), unlike SPESP1 (sperm ES protein 1), a candidate protein involved in sperm–egg fusion localized specifically in acrosome-intact ES region, which was undetectable after AR. Interestingly, our findings from MS identification also revealed that a group of heat shock proteins, such as HSPA9, HSPA8, HSPA1, HSPA2(HSP70-2, testis-specific), were associated with STK31 in testis (Table 1), coinciding with previous report that HSP70 and HSP90, together with their bound cochaperones, were critical to mediate kinase activity of TSSK6 in mice testes. We also observed that such a group of heat shock proteins were still co-immunoprecipitated in vitro when using α-STK31 antibody pull-down lysate prepared from Myc-stk31-transfected 293T cells (data not shown), suggesting heat shock proteins may be common, and pivotal players of protein kinase pathway. Altogether, these evidence suggest the significant roles of protein kinases involved in mammal reproduction, and STK31 may be a potential candidate kinase which is required for normal spermatogenesis and/or successful fertilization.

Interestingly, recent evidence showed that STK31 was also found to be expressed abundantly in colorectal cancer and gastric and esophageal cancer, and thus suggested to be a novel cancer/testis (CT) antigen (Yokoe et al. 2008; Zang et al. 2011), indicating the acquisition of a gametogenic program in cancer involved in tumorigenesis. It is also noticeable that we did not explore the expression of STK31 during mice prenatal development. The potential mechanisms and functions underlying characteristic localization of STK31 in mice testes remain to be elucidated, best through generating stk31-targeted deletion mice. Taken together, herein, our findings demonstrate, for the first time, that mouse STK31 is a potential nuage-associated component in mid-to-late spermatocytes, and its retained localization to acrosome (especially at ES) suggests that it could be a critical player at fertilization.

Acknowledgments We thank Dr. Xuemei Tong [Shanghai Jiao Tong University School of Medicine (SJTUSOM), Institute of Medical Science] for her generous gift of pIRES-Myc and pIRES -Flag plasmids. We are grateful to Qiangsu Guo and Meige Lu (Shanghai Key Lab for Reproductive Medicine), Lifang Wu (SJTUSOM, Institute of Medical Science), Guangheng Yang (SJTUSOM, Department of Developmental Biology), Jianbin Liu (SJTUSOM, Department of Medical Genetics), and Hua Sun (SJTUSOM, Cell Biology) for sharing some reagents and their technical assistance. This work was supported by grants from Shanghai Leading Academic Discipline Project (No.S30201), Shanghai Science and Technology Commission (No.10DZ2270600, 11JC1404800), and National Natural Science Foundation of China (No. 30771139, 61175024, 91130033).

Conflict of interest The authors declare no conflict of interest.

References

Bao J, Zhang J, Zheng H, Xu C, Yan W (2010) UBQLN1 interacts with SPEM1 and participates in spermiogenesis. Mol Cell Endocrinol 327:89–97

Bao J, Wu Q, Song R, Jie Z, Zheng H, Xu C, Yan W (2011) RANBP17 is localized to the XY body of spermatocytes and interacts with SPEM1 on the manchette of elongating spermatids. Mol Cell Endocrinol 333:134–142

Barsh GS, Aravin AA, van der Heijden GW, Castañeda J, Vagin VV, Hannon GJ, Bortvin A (2009) Cytoplasmic compartmentalization of the fetal piRNA pathway in mice. PLoS Genetics 5:e1000764

Carmell MA, Girard A, van de Kant HJG, Bourc'his D, Bestor TH, de Rooij DG, Hannon GJ (2007) MIWI2 is essential for spermatogenesis and repression of transposons in the mouse male germline. Developmental Cell 12:503–514

Chen C, Jin J, James DA, Adams-Cioaba MA, Park JG, Guo Y, Tenaglia E, Xu C, Gish G, Min J, Pawson T (2009) Mouse Piwi interactome identifies binding mechanism of Tdrkh Tudor domain to arginine methylated Miwi. Proc Natl Acad Sci USA 106:20336–20341

Cheng CY, Mruk DD (2011) Regulation of spermiogenesis, spermiation and blood-testis barrier dynamics: novel insights from studies on Eps8 and Arp3. Biochem J 435:553–562

Cheng D, Cote J, Shaaban S, Bedford MT (2007) The arginine methyltransferase CARM1 regulates the coupling of transcription and mRNA processing. Mol Cell 25:71–83

Chuma S, Hosokawa M, Kitamura K, Kasai S, Fujioka M, Hiyoshi M, Takamune K, Noce T, Nakatsuji N (2006) Tdrd1/Mtr-1, a tudor-related gene, is essential for male germ-cell differentiation and nuage/germinal granule formation in mice. Proc Natl Acad Sci 103:15894–15899

Cornwall GA (2009) New insights into epididymal biology and function. Hum Reprod Update 15:213–227

Drumond AL, Meistrich ML, Chiarini-Garcia H (2011) Spermatogonial morphology and kinetics during testis development in mice: a high-resolution light microscopy approach. Reproduction 142:145–155

Fujihara Y, Murakami M, Inoue N, Satouh Y, Kaseda K, Ikawa M, Okabe M (2010) Sperm equatorial segment protein 1, SPESP1, is required for fully fertile sperm in mouse. J Cell Sci 123:1531–1536

Goulet I, Boisvenue S, Mokas S, Mazroui R, Cote J (2008) TDRD3, a novel tudor domain-containing protein, localizes to cytoplasmic stress granules. Hum Mol Genet 17:3055–3074

Grivna ST (2006) MIWI associates with translational machinery and PIWI-interacting RNAs (piRNAs) in regulating spermatogenesis. Proc Natl Acad Sci 103:13415–13420

Hermo L, Pelletier RM, Cyr DG, Smith CE (2010) Surfing the wave, cycle, life history, and genes/proteins expressed by testicular germ cells. Part 2: changes in spermatid organelles associated with development of spermatozoa. Microsc Res Tech 73:279–319

Jamsai D, O'Bryan MK (2011) Mouse models in male fertility research. Asian J Androl 13:139–151

Jha KN, Wong L, Zerfas PM, De Silva RS, Fan YX, Spiridonov NA, Johnson GR (2010) Identification of a novel HSP70-binding cochaperone critical to HSP90-mediated activation of small serine/threonine kinase. J Biol Chem 285:35180–35187

Kierszenbaum AL (2006) Tyrosine protein kinases and spermatogenesis: truncation matters. Mol Reprod Dev 73:399–403

Kotaja N, Kimmins S, Brancorsini S, Hentsch D, Vonesch JL, Davidson I, Parvinen M, Sassone-Corsi P (2004) Preparation, isolation and characterization of stage-specific spermatogenic cells for cellular and molecular analysis. Nat Methods 1:249–254

Lam DM, Furrer R, Bruce WR (1970) The separation, physical characterization, and differentiation kinetics of spermatogonial cells of the mouse. Proc Natl Acad Sci USA 65:192–199

Leblond CP, Clermont Y (1952) Definition of the stages of the cycle of the seminiferous epithelium in the rat. Ann New York Acad Sci 55:548–573

Linder B, Plottner O, Kroiss M, Hartmann E, Laggerbauer B, Meister G, Keidel E, Fischer U (2008) Tdrd3 is a novel stress granule-associated protein interacting with the Fragile-X syndrome protein FMRP. Hum Mol Genet 17:3236–3246

Moser JJ, Fritzler MJ (2010) Cytoplasmic ribonucleoprotein (RNP) bodies and their relationship to GW/P bodies. Int J Biochem Cell Biol 42:828–843

Oakberg EF (1956) Duration of spermatogenesis in the mouse and timing of stages of the cycle of the seminiferous epithelium. Am J Anat 99:507–516

Pan J (2005) RNF17, a component of the mammalian germ cell nuage, is essential for spermiogenesis. Development 132:4029–4039

Russell L, Ettlin R, Sinha Hikim A, Clegg E (1990) Histological and histopathological evaluation of the testis. Cache River Press, Clearwater

Sabeur K, Ball BA, Corbin CJ, Conley A (2008) Characterization of a novel, testis-specific equine serine/threonine kinase. Mol Reprod Dev 75:867–873

Shang P, Baarends WM, Hoogerbrugge J, Ooms MP, van Cappellen WA, de Jong AA, Dohle GR, van Eenennaam H, Gossen JA, Grootegoed JA (2010) Functional transformation of the chromatoid body in mouse spermatids requires testis-specific serine/threonine kinases. J Cell Sci 123:331–339

Sipila P, Jalkanen J, Huhtaniemi IT, Poutanen M (2009) Novel epididymal proteins as targets for the development of post-testicular male contraception. Reproduction 137:379–389

Sosnik J, Miranda PV, Spiridonov NA, Yoon SY, Fissore RA, Johnson GR, Visconti PE (2009) Tssk6 is required for Izumo relocalization and gamete fusion in the mouse. J Cell Sci 122:2741–2749

Spiridonov NA, Wong L, Zerfas PM, Starost MF, Pack SD, Paweletz CP, Johnson GR (2005) Identification and characterization of SSTK, a serine/threonine protein kinase essential for male fertility. Mol Cell Biol 25:4250–4261

Tanaka T, Hosokawa M, Vagin VV, Reuter M, Hayashi E, Mochizuki AL, Kitamura K, Yamanaka H, Kondoh G, Okawa K, Kuramochi-Miyagawa S, Nakano T, Sachidanandam R, Hannon GJ, Pillai RS, Nakatsuji N, Chuma S (2011) Tudor domain containing 7 (Tdrd7) is essential for dynamic ribonucleoprotein (RNP) remodeling of chromatoid bodies during spermatogenesis. Proc Natl Acad Sci 108:10579–10584

Vagin VV, Wohlschlegel J, Qu J, Jonsson Z, Huang X, Chuma S, Girard A, Sachidanandam R, Hannon GJ, Aravin AA (2009) Proteomic analysis of murine Piwi proteins reveals a role for arginine methylation in specifying interaction with Tudor family members. Genes Dev 23:1749–1762

Vasileva A, Tiedau D, Firooznia A, Müller-Reichert T, Jessberger R (2009) Tdrd6 is required for spermiogenesis, chromatoid body architecture, and regulation of miRNA expression. Curr Biol 19:630–639

Wang S (2005) Cullin3 is a KLHL10-interacting protein preferentially expressed during late spermiogenesis. Biol Reprod 74:102–108

Wang PJ, McCarrey JR, Yang F, Page DC (2001) An abundance of X-linked genes expressed in spermatogonia. Nat Genet 27:422–426

Wang J, Saxe JP, Tanaka T, Chuma S, Lin H (2009) Mili interacts with tudor domain-containing protein 1 in regulating spermatogenesis. Curr Biol 19:640–644

Wu JY, Ribar TJ, Cummings DE, Burton KA, McKnight GS, Means AR (2000) Spermiogenesis and exchange of basic nuclear proteins are impaired in male germ cells lacking Camk4. Nat Genet 25:448–452

Xu B, Hao Z, Jha KN, Zhang Z, Urekar C, Digilio L, Pulido S, Strauss Iii JF, Flickinger CJ, Herr JC (2008) Targeted deletion of Tssk1 and 2 causes male infertility due to haploinsufficiency. Dev Biol 319:211–222

Yabuta Y, Ohta H, Abe T, Kurimoto K, Chuma S, Saitou M (2011) TDRD5 is required for retrotransposon silencing, chromatoid body assembly, and spermiogenesis in mice. J Cell Biol 192:781–795

Yan W (2009) Male infertility caused by spermiogenic defects: lessons from gene knockouts. Mol Cell Endocrinol 306:24–32

Yang Y, Lu Y, Espejo A, Wu J, Xu W, Liang S, Bedford MT (2010) TDRD3 is an effector molecule for arginine-methylated histone marks. Mol Cell 40:1016–1023

Yokoe T, Tanaka F, Mimori K, Inoue H, Ohmachi T, Kusunoki M, Mori M (2008) Efficient identification of a novel cancer/testis antigen for immunotherapy using three-step microarray analysis. Cancer Res 68:1074–1082

Yoshida S, Sukeno M, Nakagawa T, Ohbo K, Nagamatsu G, Suda T, Nabeshima Y (2006) The first round of mouse spermatogenesis is a distinctive program that lacks the self-renewing spermatogonia stage. Development 133:1495–1505

Zang ZJ, Ong CK, Cutcutache I, Yu W, Zhang SL, Huang D, Ler LD, Dykema K, Gan A, Tao J, Lim S, Liu Y, Futreal PA, Grabsch H, Furge KA, Goh LK, Rozen S, Teh BT, Tan P (2011) Genetic and structural variation in the gastric cancer kinome revealed through targeted deep sequencing. Cancer Res 71:29–39

Zuercher G, Rohrbach V, Andres AC, Ziemiecki A (2000) A novel member of the testis specific serine kinase family, tssk-3, expressed in the Leydig cells of sexually mature mice. Mech Dev 93:175–177